

Article

Aluminum Foam-Filled Steel Tube Fabricated from Aluminum Burrs of Die-Castings by Friction Stir Back Extrusion

Yoshihiko Hangai ^{1,*}, Ryusei Kobayashi ¹, Ryosuke Suzuki ¹, Masaaki Matsubara ¹
and Nobuhiro Yoshikawa ²

¹ Faculty of Science and Technology, Gunma University, Kiryu 376-8515, Japan; t13302045@gunma-u.ac.jp (R.K.); r_suzuki@gunma-u.ac.jp (R.S.); m.matsubara@gunma-u.ac.jp (M.M.)

² Institute of Industrial Science, The University of Tokyo, Tokyo 153-8505, Japan; nobuyoshi@iis.u-tokyo.ac.jp

* Correspondence: hanhan@gunma-u.ac.jp

Received: 30 December 2018; Accepted: 18 January 2019; Published: 24 January 2019



Abstract: A mixture of Al burrs of Al high-pressure die-castings and a blowing agent powder was used to fabricate Al foam-filled steel tubes by friction stir back extrusion (FSBE). It was shown that the mixture can be sufficiently consolidated to form an Al precursor that is coated on the inner surface of a steel tube by the plastic flow generated during FSBE. Namely, a precursor coated steel tube can be fabricated from Al burrs by FSBE. By heat treatment of the precursor coated steel tube, an Al foam-filled steel tube can be fabricated. Al foam was sufficiently filled in the steel tube, and the porosity was almost homogeneously distributed in the entire sample. In compression tests of the samples, the Al foam-filled steel tube fabricated from Al burrs exhibited similar compression properties to an Al foam-filled steel tube fabricated from the bulk Al precursor. Consequently, it was shown that an Al foam-filled steel tube cost-effectively fabricated from Al burrs by FSBE compares favorably with an Al foam-filled steel tube fabricated from the bulk Al precursor.

Keywords: cellular materials; composites; friction welding; foam; recycle

1. Introduction

Composite structures consisting of a dense metallic tube filled with aluminum (Al) foam have attracted interest in various industrial fields owing to their light-weight and good energy absorption properties [1,2]. Generally, Al foam-filled metallic tubes have been fabricated by simply placing Al foam into a metallic tube with a gap between the Al foam and the metallic tube, which adversely affects the mechanical properties of the tube [3,4]. Hamada et al. and Toksoy et al. demonstrated that bonding between the Al foam and Al tube with adhesives resulted in superior absorption properties to those without any bonding [3,5]. Bonaccorsi et al. fabricated an Al foam-filled steel tube with metal bonding between the Al foam and steel tube by foaming a precursor in the steel tube [6]. The precursor was a solid Al homogeneously containing blowing agent [7,8]. Duarte et al. fabricated an Al foam-filled Al tube with metal bonding between the Al foam and Al tube by foaming a precursor in the Al tube [9].

Friction stir back extrusion (FSBE) has been developed for coating wear-resistant Al-25%Si on the surface of an Al-Si-Cu alloy AC2B engine cylinder [10], and for fabricating Al tubes and copper tubes with a fine grain structure from bulk starting materials [11,12]. Hangai et al. developed a fabrication process for Al foam-filled steel tubes [13,14] and Al foam-filled Al tubes [15,16] by FSBE. In this process, a bulk Al precursor was placed into a metal tube; then a rotating tool was plunged onto the precursor. The generated friction heat between the rotating tool and precursor softened the precursor, then the plastic flow of the precursor occurred, causing it to fill the space between the rotating tool and the

metal tube, resulting in the coating of the precursor on the surface of the metal tube. The plastic flow induced the exposure of the new surface of the precursor and metal tube, realizing strict contact between them. Heat treatment of the precursor resulted in the foaming of the precursor, which filled the tube and bonded to the tube with metallic bonding. A bilayer tube consisting of an outer Al foam and an inner Al tube can also be fabricated by a similar process [17].

A reduction in cost and the high recyclability of Al foam-filled metal tubes can be expected by using Al chip waste from industrial production [18,19]. Consolidation of Al chips has been attempted by hot extrusion [18,19], compression torsion processing [20,21], friction extrusion [22], friction consolidation [23–25], screw extrusion [26], and FSBE [27]. Among these processes, FSBE can fabricate an Al tube directly from Al chips and realize strict contact with an outer metal tube.

In this study, a mixture of Al burrs of Al high-pressure die-castings and a blowing agent powder was used to fabricate Al foam-filled steel tubes by FSBE. It was expected that a foamable precursor would be fabricated by consolidating the mixture by the plastic flow generated during FSBE, along with the coating of the precursor on the inner surface of the steel tube. By heat treatment of the precursor coated steel tubes, Al foam-filled steel tubes were obtained. The pore structures of the inner Al foam were nondestructively observed to determine whether sufficient foaming occurred, and the pores were found to be homogeneously distributed in the whole specimen. Thereafter, compression tests of the obtained Al foam-filled steel tubes were conducted to determine whether similar mechanical properties to those of an Al foam-filled tube fabricated from the bulk Al precursor could be obtained.

2. Materials and Methods

2.1. Fabrication of Al Foam-Filled Steel Tube

Figure 1 shows Al burrs used to fabricate the Al foam of the Al foam-filled steel tube. The Al burrs were from Al-Si-Cu alloy ADC12 (equivalent to A383.0 Al alloy) die-castings. Figure 1a shows a scanning electron microscope (JEOL Ltd., Tokyo, Japan) image of the ADC12 burrs in powder form. As received ADC12 burrs were sieved with a mesh size of 180 μm to remove the impurities and for easy mixing with the blowing agent powder. Figure 1b shows the ADC12 burrs in round-plate form. Relatively thick (approximately 0.2 mm thickness) ADC12 burrs were cut into a circular shape with a diameter of 18 mm.

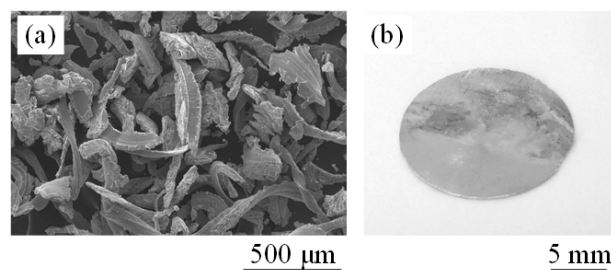


Figure 1. ADC12 burrs (a) in powder form and (b) in round-plate form.

Figure 2 shows the fabrication process of the Al foam-filled steel tube by FSBE. First, as shown in Figure 2a, ADC12 burrs in powder form and a blowing agent powder were mixed. TiH_2 powder (<45 μm) was used as the blowing agent. The amount of TiH_2 was one mass% relative to the mass of ADC12 burrs in accordance with reference [13]. As shown in Figure 2b, the mixture was placed in a SUS304 stainless-steel tube fixed by a steel jig. The steel tube had a diameter of 20 mm, a thickness of 0.2 mm, and 40 mm height. Then, five ADC12 burrs in round-plate form were laminated on top of the mixture in the steel tube to prevent the mixture from scattering during FSBE. As shown in Figure 2c, a rotating tool was plunged from above until the tip of the tool reached 3 mm above the bottom of the steel tube using friction stir welding machine (Hitachi Setsubi Engineering Co., Ltd., Hitachi, Japan). The rotation speed and plunging rates were 1500 rpm and 4 mm/min, respectively. The tool was made

of tool steel with a diameter of 16 mm and had a flat bottom. The mixture was consolidated by loading the tool and the plastic flow of the mixture, resulting in the formation of a precursor and the coating on the inner surface of the steel tube. The temperature during the plunging of the tool was obtained by a K-type thermocouple placed at half the height of the steel tube and 2 mm from its surface. As shown in Figure 2d, the upper and lower parts of the obtained precursor coated steel tube were machined by wire electrical discharge machining, then the entire tube was foamed by heat treatment in an electric furnace previously held at 675 °C for 6.5–7.0 min. Then, as shown in Figure 2e, an Al foam-filled steel tube was obtained. The upper and lower parts of the obtained Al foam-filled steel tube were machined by wire electrical discharge machining to obtain a compression test specimen with 20 mm diameter and 20 mm height. Fourteen compression test specimens were obtained. In addition, similar compression test specimens were fabricated from a bulk Al precursor, which was fabricated by the friction stir welding route [28,29], by the same process as above using FSBE.

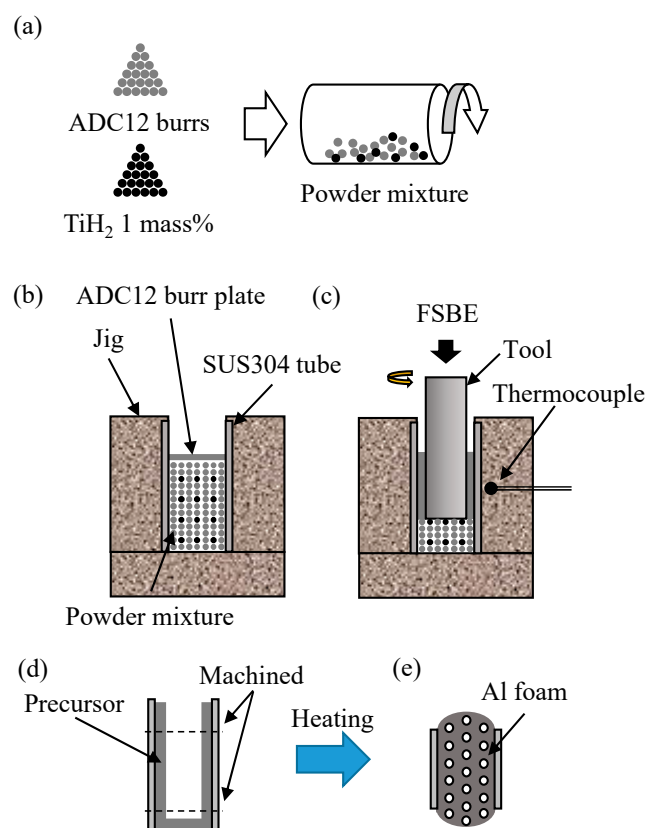


Figure 2. Schematic illustration of fabrication process of Al foam-filled steel tube by FSBE.

2.2. Evaluation of Pore Structures

The pore structures of the compression test specimens were nondestructively observed by a microfocus X-ray CT system (Shimadzu Corporation, Kyoto, Japan) at room temperature in accordance with reference [30]. The X-ray source was tungsten. A cone-beam CT system, where only one rotation of the specimen is required to obtain a set of cross-sectional X-ray CT images with the slice pitch equal to the length of one pixel in the CT image, was employed. The number of slices was about 450. The voltage and current of the X-ray tube were 80 kV and 30 μ A, respectively. The equivalent length of a pixel was approximately 74 μ m.

The porosity (volume fraction of pores) p (%) of the Al foam part of each compression test specimen was evaluated as follows. First, the density of the Al foam part ρ_f was evaluated as

$$\rho_f = \frac{m_{\text{FFT}} - m_{\text{tube}}}{V_{\text{FFT}} - V_{\text{tube}}},$$

where m_{FFT} and V_{FFT} are the mass and volume of the compression test specimen, respectively, which were obtained from the measured weight and dimensions of the specimen. m_{tube} and V_{tube} are the mass and volume of the steel tube part of the compression test specimen, respectively. Then, p was evaluated as

$$p = \frac{\rho_i - \rho_f}{\rho_i} \times 100,$$

where ρ_i is the density of the precursor without the tube before foaming, for which the density of ADC12 Al alloy [31] was used.

2.3. Compression Tests

Compression tests of the obtained Al foam-filled steel tubes were conducted using a universal testing machine (Shimadzu Corporation, Kyoto, Japan). The compression rate was 4 mm/min in accordance with reference [32]. The compression stress was obtained by dividing the compression load by the area of the circle equivalent to the outer diameter of the Al foam-filled steel tube.

3. Results and Discussion

3.1. Time–Temperature Relationship during FSBE

Figure 3 shows typical relationships obtained between torque N and time t and between temperature T and time t . $t = 0$ was defined as the time when the tool first came in contact with the ADC12 burrs in the round-plate form. As the indentation of the tool increased, the ADC12 burrs were densified, and plastic flow occurred. It has been reported that the filling of the Al between the rotating tool and tube occurs from the upper part, which is softened by the friction heat generated between the rotating tool and the Al precursor [15]. It is considered that plastic flow occurred in the vicinity of the tool where friction heat was generated. The torque and temperature gradually increased in this stage. At around $t = 5$ min, the torque increased rapidly. The temperature exhibited a similar tendency except with a small delay due to the time for the generated heat to be transferred to the thermocouple. In this stage, densification of the ADC12 burrs had finished, and only plastic flow occurred, resulting in a rapid increase in the resistance force and temperature. Similar tendencies were observed for all other samples, and the maximum temperatures of all the samples were between 350 and 415 °C. Also, similar tendencies were observed for the samples using the bulk Al precursor. These temperatures are much lower than the solidus temperature of ADC12 (515 °C [31]), at which the foaming of the precursor begins [33,34]. It has been demonstrated that the decomposition of TiH_2 gradually occurs between 390 and 920 °C [35], 427 and 850 °C [36], and 440 and 800 °C [37]. In the FSBE process, it is assumed that little decomposition of TiH_2 occurred because the temperature of the precursor reached these reported decomposition temperatures for only a limited time. Therefore, almost all the TiH_2 remained without decomposition.

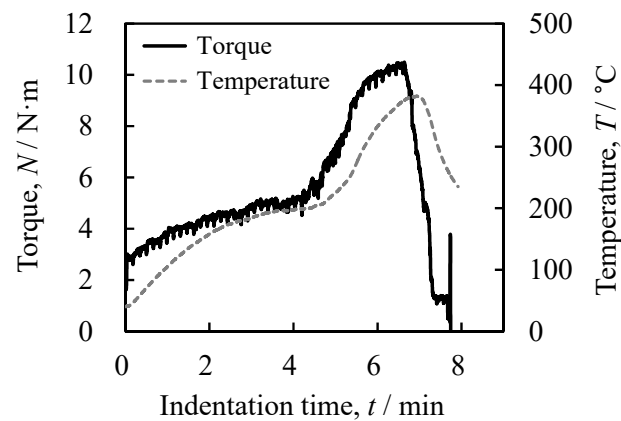


Figure 3. Torque N – indentation time t and temperature T – t relationships during FSBE.

3.2. Obtained Al Foam-Filled Steel Tube

Figure 4a shows the as-fabricated precursor coated tube. It was shown that the ADC12 burrs were sufficiently consolidated except in the upper part of the tube. The upper part of the tube was subjected to a less plastic flow during FSBE, resulting in insufficient consolidation of the ADC12 burrs. These parts were machined before foaming as shown in Figure 4b. Figure 4c shows a cross-section of the machined precursor before foaming, and Figure 4d shows an enlarged image of the bonding region of Figure 4c. It was shown that the ADC12 burrs were sufficiently consolidated to form the precursor and were coated on the surface of the tube without a gap between the tube and precursor by the load of the tool and the intense plastic flow during the FSBE.

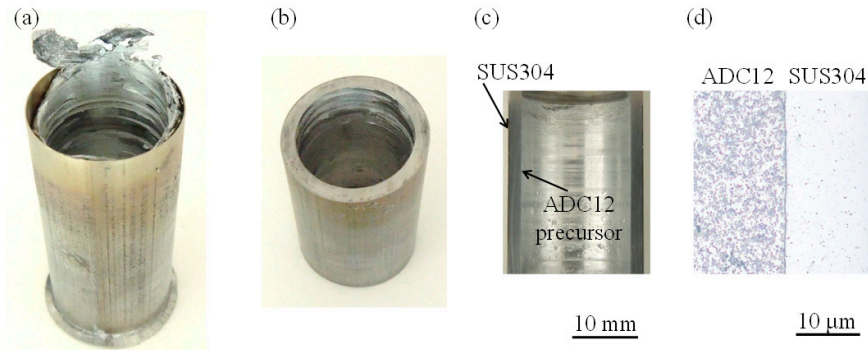


Figure 4. (a) As-fabricated precursor-coated steel tube. (b) machined precursor-coated steel tube before foaming and (c) its cross section. (d) enlarged image of bonding region of (c).

Figure 5a,b show the as-foamed Al foam-filled steel tubes after foaming for 6.5 min and 7.0 min, Figure 5c,d show the Al foam-filled steel tube compression test specimens obtained by machining the samples shown in Figure 5a,b, and Figure 5e,f show their cross-sectional X-ray CT images, respectively. Black and white regions in the X-ray CT images indicate pores and Al, respectively. Although a few large pores were observed, it was shown that the coated precursor was sufficiently foamed and filled the tubes. The porosities of the Al foam part of the compression test specimens shown in Figure 5c,d were $p = 79.3\%$ and $p = 90.2\%$, respectively.

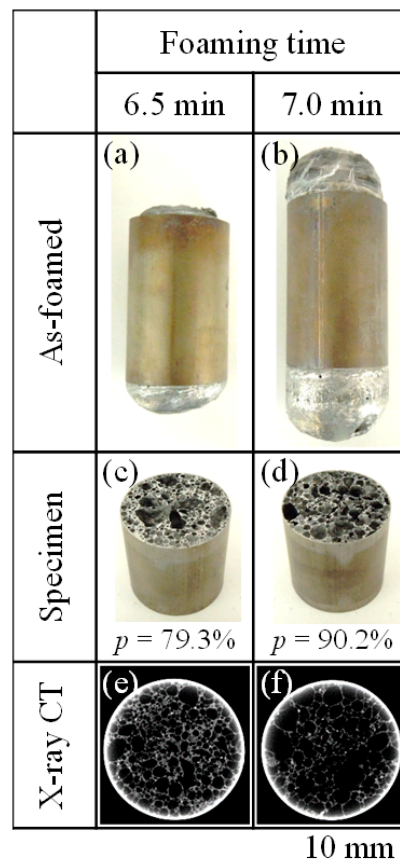


Figure 5. (a,b) As-foamed Al foam-filled steel tubes after foaming for 6.5 min and 7.0 min, respectively. (c,d) Al foam-filled steel tube compression test specimens machined from (a,b), respectively. (e,f) Their cross-sectional X-ray CT images.

Figure 6 shows the relationship between the porosity and foaming time of all the compression test specimens. The figure indicates that vigorous foaming occurred between 6.5 min and 7.0 min. In previous studies on the foaming of ADC12 precursor [33,34], it was demonstrated that the precursor started to foam once the precursor temperature exceeded the solidus temperature and gradually foamed between the solidus and liquidus temperatures. Then, vigorous foaming occurred once the precursor temperature exceeded the liquidus temperature. Although some variation among the porosities appeared at a foaming time of 6.5 min owing to the difficulty of obtaining the same foaming behavior for each specimen using an electric furnace, a foaming time of around 7.0 min induced sufficient foaming for the precursor temperature of all the samples to exceed the liquidus temperature.

Figure 7 shows the porosity distributions of the compression test specimens shown in Figure 5c,d in the height direction for foaming times of 6.5 min ($p = 79.3\%$) and 7.0 min ($p = 90.2\%$), respectively, which were evaluated using X-ray CT images such as shown in Figure 5e,f by image processing software. Although there were a few large pores, the Al foam sufficiently filled the tube with an almost homogeneous porosity distribution throughout the entire specimen, especially for the sample foamed for 7.0 min, which exhibited sufficient foaming of the precursor. The variation of the porosity and the existence of large pores are considered to be due to the insufficient distribution of the foaming agent compared with that in the bulk precursor because it was difficult to homogeneously mix the ADC12 burr and TiH_2 powders with different particle sizes. Also, slight segregation occurred during the insertion of the mixture into the tube and during the FSBE. This may be prevented by using ADC12 burr particles with a similar size to that of TiH_2 .

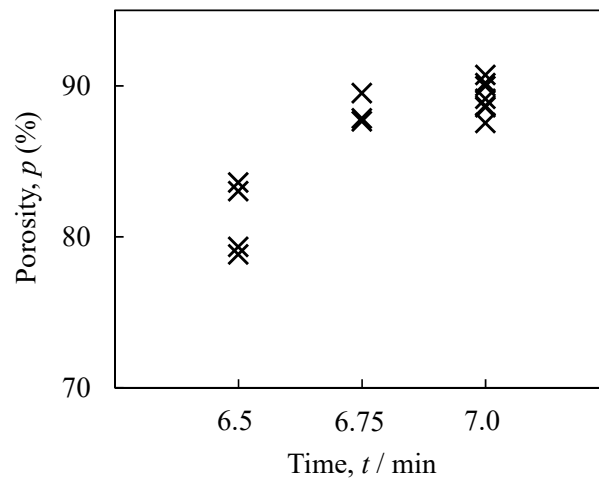


Figure 6. Relationship between porosity and foaming time of obtained Al foam-filled steel tube compression test specimens.

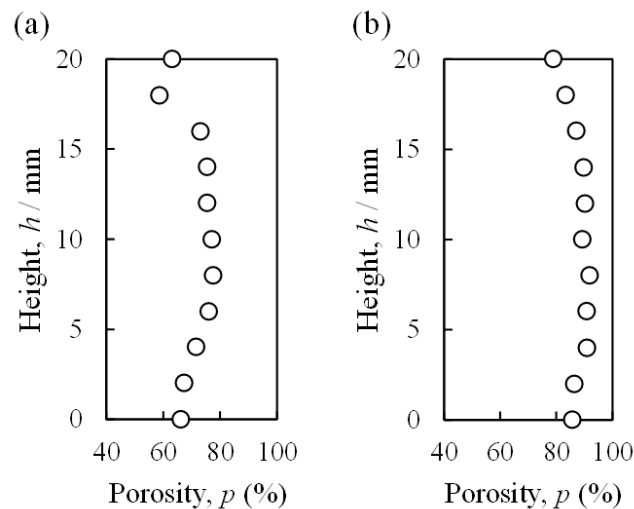


Figure 7. Porosity distributions in the height direction of Al foam-filled steel tube compression test specimens with (a) $p = 79.3\%$ and (b) $p = 90.2\%$ corresponding to Figure 5c,d, respectively.

3.3. Compression Properties

Figure 8 shows the deformation behavior of the fabricated Al foam-filled steel tubes with $p = 79.3\%$ and $p = 90.2\%$, respectively, which are shown in Figure 5c,d during the compression test, along with that of the tube fabricated from the bulk Al precursor with $p = 84.5\%$ by FSBE in accordance with Ref. [13]. The three black lines on the surface of the samples perpendicular to the compression direction were marks made to easily observe the deformation behavior. It was found that the deformation occurred layer by layer. Little difference was observed in the deformation behavior between the Al foams with different porosities, although the number of buckling folds were different. This difference is because the lower-porosity Al foam expanded in the width direction as the deformation increased. In contrast, the higher-porosity Al foam deformed with little expansion in the width direction. The deformation behavior was similar for the other specimens fabricated in this study, including those fabricated from the bulk Al precursor.

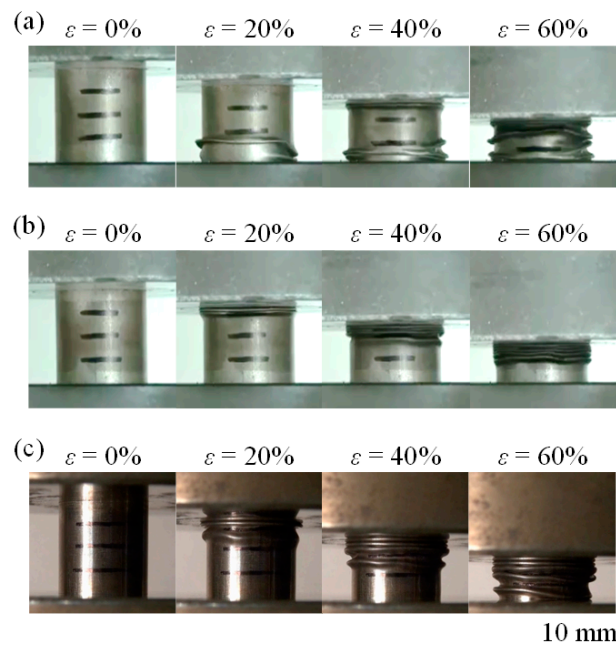


Figure 8. Deformation behavior during compression test of the fabricated Al foam-filled steel tube with (a) $p = 79.3\%$, corresponding to Figure 5b,c. (b) $p = 90.2\%$, corresponding to Figure 5d,c Al foam-filled steel tube fabricated using bulk Al precursor with (c) $p = 84.5\%$.

Figure 9 shows the stress σ – strain ε curves of the fabricated Al foam-filled steel tubes with $p = 79.3\%$ and $p = 90.2\%$; along with that of the tube fabricated from the bulk Al precursor with $p = 84.5\%$, whose deformation behavior is shown in Figure 8. An elastic region in the early stage of the σ – ε curves, where σ rapidly increased to an initial maximum stress was observed. Then, a plateau region exhibiting an appropriately constant or slightly increasing σ was observed as ε increased. Then, a densification region where σ rapidly increased was observed. The increases and decreases in σ in the plateau region were observed when the folds were generated. These σ – ε curves were also observed for other specimens fabricated in this study regardless of the porosity.

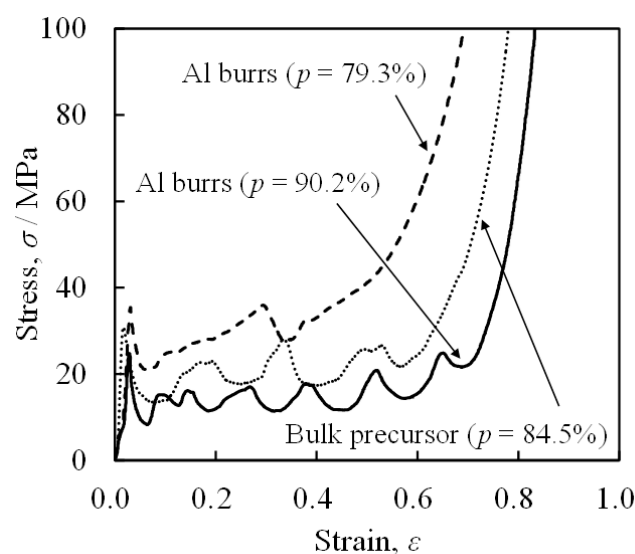


Figure 9. Stress–strain curves for the specimens in Figure 8.

Figure 10 shows the plateau stress σ_{pl} – porosity p and energy absorption per unit volume E_V – porosity p relationships for all the samples including those fabricated from the bulk Al precursor. σ_{pl} was defined as the average σ for $\varepsilon = 0.2$ – 0.3 in the σ – ε curves and E_V was defined as the area under the σ – ε curves for $\varepsilon = 0$ – 0.5 in accordance with Ref. 32. It was found that σ_{pl} and E_V decreased as p increased. This tendency was also observed for the samples fabricated from the bulk Al precursor. Consequently, it was shown that Al foam-filled steel tubes can be fabricated from ADC12 burrs that exhibit almost the same compression properties as Al foam-filled steel tubes fabricated from the bulk Al precursor when the porosity of the Al foam part is the same.

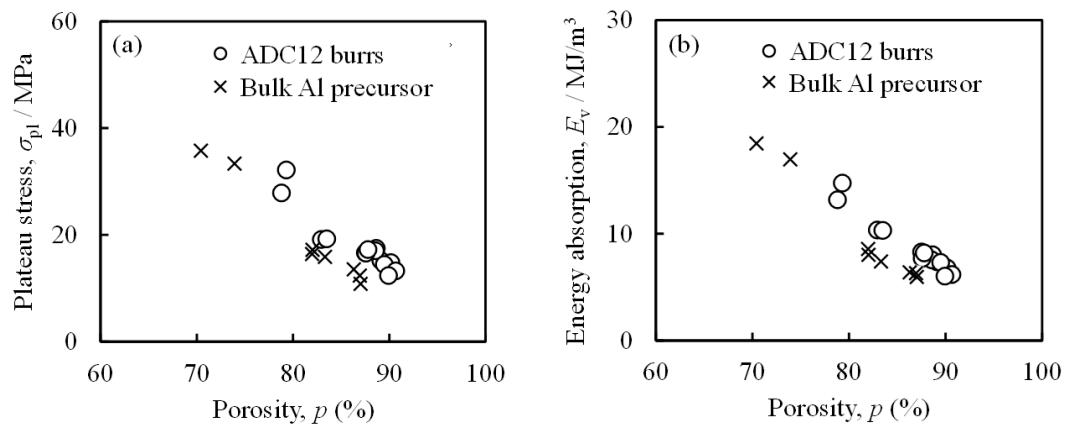


Figure 10. Relationship between (a) plateau stress σ_{pl} and (b) energy absorption per unit volume E_V and porosity p for the obtained Al foam-filled steel tubes fabricated from ADC12 burrs along with those fabricated from the bulk Al precursor.

4. Conclusions

In this study, a mixture of ADC12 burrs of Al high-pressure die-castings and a blowing agent powder was used to fabricate Al foam-filled steel tubes by FSBE. The experimental results led to the following conclusions.

(1) A mixture of ADC12 burrs and a blowing agent can be sufficiently consolidated to form a precursor that is coated on the inner surface of a steel tube by FSBE. Namely, a precursor-coated steel tube can be fabricated from ADC12 burrs by FSBE.

(2) An Al foam-filled steel tube can be fabricated by heat treatment of the precursor coated steel tube. Al foam was sufficiently filled in the steel tube, and the porosity was almost homogeneously distributed in the entire sample.

(3) The Al foam-filled steel tube fabricated from ADC12 burrs exhibited similar compression properties to an Al foam-filled steel tube fabricated from the bulk Al precursor.

Consequently, it was shown that an Al foam-filled steel tube can be cost-effectively fabricated from Al burrs by FSBE and compares favorably with an Al foam-filled steel tube fabricated from the bulk Al precursor.

Author Contributions: Y.H. elaborated the research idea and wrote this manuscript. R.K. and R.S. performed the experimental work and contributed to the discussion of the experimental results. M.M. and N.Y. performed literature review and contributed to the discussion of the experimental results.

Conflicts of Interest: The authors declare no conflict of interest.

References

- Banhart, J. Manufacture, characterisation and application of cellular metals and metal foams. *Prog. Mater. Sci.* **2001**, *46*, 559–632. [[CrossRef](#)]
- García-Moreno, F. Commercial applications of metal foams: Their properties and production. *Materials* **2016**, *9*, 85. [[CrossRef](#)] [[PubMed](#)]

3. Hamada, T.; Kanahashi, H.; Kanetake, N. Axial crushing performance of porous aluminum filled members. *J. Jpn. Inst. Met. Mater.* **2009**, *73*, 453–461. [[CrossRef](#)]
4. Duarte, I.; Vesenjaj, M.; Krstulović-Opara, L. Dynamic and quasi-static bending behaviour of thin-walled aluminium tubes filled with aluminium foam. *Compos. Struct.* **2014**, *109*, 48–56. [[CrossRef](#)]
5. Toksoy, A.K.; Tanoglu, M.; Guden, M.; Hall, I.W. Effect of adhesive on the strengthening of aluminum foam-filled circular tubes. *J. Mater. Sci.* **2004**, *39*, 1503–1506. [[CrossRef](#)]
6. Bonaccorsi, L.; Proverbio, E.; Raffaele, N. Effect of the interface bonding on the mechanical response of aluminium foam reinforced steel tubes. *J. Mater. Sci.* **2010**, *45*, 1514–1522. [[CrossRef](#)]
7. Baumgartner, F.; Duarte, I.; Banhart, J. Industrialization of powder compact foaming process. *Adv. Eng. Mater.* **2000**, *2*, 168–174. [[CrossRef](#)]
8. Hangai, Y.; Utsunomiya, T.; Hasegawa, M. Effect of tool rotating rate on foaming properties of porous aluminum fabricated by using friction stir processing. *J. Mater. Process. Technol.* **2010**, *210*, 288–292. [[CrossRef](#)]
9. Duarte, I.; Vesenjaj, M.; Krstulovic-Opara, L.; Ren, Z.R. Static and dynamic axial crush performance of in-situ foam-filled tubes. *Compos. Struct.* **2015**, *124*, 128–139. [[CrossRef](#)]
10. Shinoda, T. Applications of friction technology on cast materials. *J. JFS* **2011**, *83*, 695–701.
11. Abu-Farha, F. A preliminary study on the feasibility of friction stir back extrusion. *Scr. Mater.* **2012**, *66*, 615–618. [[CrossRef](#)]
12. Dinaharan, I.; Sathiskumar, R.; Vijay, S.J.; Murugan, N. Microstructural Characterization of pure copper tubes produced by a novel method friction stir back extrusion. *Procedia Mater. Sci.* **2014**, *5*, 1502–1508. [[CrossRef](#)]
13. Hangai, Y.; Saito, M.; Utsunomiya, T.; Kitahara, S.; Kuwazuru, O.; Yoshikawa, N. Fabrication of aluminum foam-filled thin-wall steel tube by friction welding and its compression properties. *Materials* **2014**, *7*, 6796–6810. [[CrossRef](#)]
14. Hangai, Y.; Nakano, Y.; Utsunomiya, T.; Kuwazuru, O.; Yoshikawa, N. Drop weight impact behavior of Al-Si-Cu alloy foam-filled thin-walled steel pipe fabricated by friction stir back extrusion. *J. Mater. Eng. Perform.* **2017**, *26*, 894–900. [[CrossRef](#)]
15. Hangai, Y.; Nakano, Y.; Koyama, S.; Kuwazuru, O.; Kitahara, S.; Yoshikawa, N. Fabrication of aluminum tubes filled with aluminum alloy foam by friction welding. *Materials* **2015**, *8*, 7180–7190. [[CrossRef](#)] [[PubMed](#)]
16. Hangai, Y.; Otazawa, S.; Utsunomiya, T. Aluminum alloy foam-filled aluminum tube fabricated by friction stir back extrusion and its compression properties. *Compos. Struct.* **2018**, *183*, 416–422. [[CrossRef](#)]
17. Hangai, Y.; Otazawa, S.; Utsunomiya, T.; Suzuki, R.; Koyama, S.; Matsubara, M.; Yoshikawa, N. Fabrication of bilayer tube consisting of outer aluminum foam tube and inner dense aluminum tube by friction stir back extrusion. *Mater. Today Commun.* **2018**, *15*, 36–42. [[CrossRef](#)]
18. Gronostajski, J.Z.; Kaczmar, J.W.; Marciniak, H.; Matuszak, A. Direct recycling of aluminium chips into extruded products. *J. Mater. Process. Technol.* **1997**, *64*, 149–156. [[CrossRef](#)]
19. Tekkaya, A.E.; Schikorra, M.; Becker, D.; Biermann, D.; Hammer, N.; Pantke, K. Hot profile extrusion of AA-6060 aluminum chips. *J. Mater. Process. Technol.* **2009**, *209*, 3343–3350. [[CrossRef](#)]
20. Kanetake, N.; Kobashi, M.; Tsuda, S. Foaming behavior of aluminum precursor produced from machined chip waste. *Adv. Eng. Mater.* **2008**, *10*, 840–844. [[CrossRef](#)]
21. Takahashi, T.; Kume, Y.; Kobashi, M.; Kanetake, N. Solid state recycling of aluminum machined chip wastes by compressive torsion processing. *J. Japan Inst. Light Met.* **2009**, *59*, 354–358. [[CrossRef](#)]
22. Tang, W.; Reynolds, A.P. Production of wire via friction extrusion of aluminum alloy machining chips. *J. Mater. Process. Technol.* **2010**, *210*, 2231–2237. [[CrossRef](#)]
23. Tang, W.; Reynolds, A.P. *Friction Consolidation of Aluminum Chips*; John Wiley & Sons: Chichester, UK, 2011; pp. 289–298.
24. Hagihara, M.; Katoh, K.; Maeda, M.; Nomoto, M. Effect of chip shape on frictional consolidated 2017 aluminum alloy chips. In Proceedings of the 129th Conference of Japan Institute of Light Metals, Tsudanuma, Japan, 21 November 2015; pp. 215–216.
25. Li, X.; Baffari, D.; Reynolds, A.P. Friction stir consolidation of aluminum machining chips. *Int. J. Adv. Manuf. Technol.* **2018**, *94*, 2031–2042. [[CrossRef](#)]
26. Wideroe, F.; Welo, T. Using contrast material techniques to determine metal flow in screw extrusion of aluminium. *J. Mater. Process. Technol.* **2013**, *213*, 1007–1018. [[CrossRef](#)]

27. Hangai, Y.; Kobayashi, R.; Suzuki, R.; Matsubara, M.; Yoshikawa, N. Fabrication of aluminum pipe from aluminum chips by friction stir back extrusion. *J. Jpn. Inst. Met. Mater.* **2018**, *82*, 33–38. [[CrossRef](#)]
28. Hangai, Y.; Ozeki, Y.; Utsunomiya, T. Foaming conditions of porous aluminum in fabrication of ADC12 aluminum alloy die castings by friction stir processing. *Mater. Trans.* **2009**, *50*, 2154–2159. [[CrossRef](#)]
29. Hangai, Y.; Takada, K.; Endo, R.; Fujii, H.; Aoki, Y.; Utsunomiya, T. Foaming of aluminum foam precursor during friction stir welding. *J. Mater. Process. Technol.* **2018**, *259*, 109–115. [[CrossRef](#)]
30. Hangai, Y.; Takahashi, K.; Yamaguchi, R.; Utsunomiya, T.; Kitahara, S.; Kuwazuru, O.; Yoshikawa, N. Nondestructive observation of pore structure deformation behavior of functionally graded aluminum foam by X-ray computed tomography. *Mater. Sci. Eng. A* **2012**, *556*, 678–684. [[CrossRef](#)]
31. The-Japan-Institute-of-Light-Metals. *Structures and Properties of Aluminum*; The Japan Institute of Light Metals: Tokyo, Japan, 1991.
32. JIS-H-7902. *Method for Compressive Test of Porous Metals*; Japanese Standards Association: Tokyo, Japan, 2016.
33. Hangai, Y.; Amagai, K.; Tsurumi, N.; Omachi, K.; Shimizu, K.; Akimoto, K.; Utsunomiya, T.; Yoshikawa, N. Forming of aluminum foam using light-transmitting material as die during foaming by optical heating. *Mater. Trans.* **2018**, *59*, 1854–1859. [[CrossRef](#)]
34. Hangai, Y.; Amagai, K.; Omachi, K.; Tsurumi, N.; Utsunomiya, T.; Yoshikawa, N. Forming of aluminum foam using steel mesh as die during foaming of precursor by optical heating. *Opt. Laser Technol.* **2018**, *108*, 496–501. [[CrossRef](#)]
35. Matijasevic-Lux, B.; Banhart, J.; Fiechter, S.; Görke, O.; Wanderka, N. Modification of titanium hydride for improved aluminium foam manufacture. *Acta Mater.* **2006**, *54*, 1887–1900. [[CrossRef](#)]
36. Illeková, E.; Harnúšková, J.; Florek, R.; Simančík, F.; Maťko, I.; Švec, P. Peculiarities of TiH₂ decomposition. *J. Therm. Anal. Calorim.* **2011**, *105*, 583–590. [[CrossRef](#)]
37. Peng, Q.; Yang, B.; Friedrich, B. Porous Titanium Parts Fabricated by Sintering of TiH₂ and Ti Powder Mixtures. *J. Mater. Eng. Perform.* **2018**, *27*, 228–242. [[CrossRef](#)]



© 2019 by the authors. Licensee MDPI, Basel, Switzerland. This article is an open access article distributed under the terms and conditions of the Creative Commons Attribution (CC BY) license (<http://creativecommons.org/licenses/by/4.0/>).